International Journal of Engineering and Applied Sciences (IJEAS)
Vol.1, Issue 2(2009)16-32

REFINED NON-CONFORMING FIVE-NODE THIN FLAT SHELL ELEMENT

H. Gedikli and H. Sofuoğlu
Karadeniz Technical University, Depertmant of Mechanical Engineering, Trabzon-TURKIYE
E-mail: hgedikli@ktu.edu.tr

Accepted Date: 04 June 2009

Abstract

In this study, a new 5-node discrete Kirchhoff flat shell element with 30 degrees of freedom (dof), called DKP30, was proposed. This element was developed by superposing the15-dof membrane element and the 15-dof plate bending element at the element level. In developing procedure Allmansi interpolation function was utilized for drilling dof of the membrane element while the plate bending element was derived via discrete Kirchhoff plate formulation. In order to test its performance the patch test was first applied to the DKP30 element and it was then subjected to the standard test problems and compared with the shell elements available in the literature. The numerical results showed that the proposed 5-node thin flat shell element, DKP30, passed the patch test and presented moderate accuracy and high performance while its usage as a transition element with a 4-node DKQ24 thin flat shell element was also found to be possible.

Key Words: 5-node Membrane Element, 5-node Plate Bending Element, 5-node Flat Shell Element, Discrete Kirchhoff Formulation.

1. Introduction

Because the formulation of the plate/shell finite elements is an important and relatively difficult subject, finite element analysis of plate/shell has been receiving continuous attention since the early days of the development of this method. In the literature, a great number of papers dealing with shell elements have been published for linear and non-linear analysis. Recently, a detailed review of shell elements available in the literature has been given in [1]. Generally, shell elements can be classified into three categories: curved elements, isoparametric curved elements (degenerated elements) and flat plate/shell elements [2, 3]. The important models for shell elements were developed since last 40 years and they were applied to the practical problems. Unfortunately, among all these models there would not be a model which was general and wide enough to simulate every individual problem. Therefore, the most closely and correctly simulating one are chosen to be used to simulate the real problems.
The flat shell element type was the first finite element shell analysis to approximate the true shell shape. In this method, the membrane and bending stiffness are superposed at the element level and the coupling between them was provided by transforming the local degree of freedom (dof) to the global ones. The flat shell elements are widely used in engineering practice due to the simplicity of the formulation, the effectiveness of the computation and the flexibility in applications. T12 [4] element obtained by superposition of the constant strain triangle (CST) and the Morley [5] triangular flat shell element. During the years, many flat shell triangular elements have been presented, such as DKT12 ve DKT15 [6], DKT18 [7, 8], DLR18 [9], DKT27 [10,11,12], DKT24 [13], HCT18 [14], HSM18 [15], TRUNC [16] and TRIC [17]. Moreover, 4-node quadrilateral DKQ16 element was also proposed by Batoz and

his co-workers [3] as well as triangular flat shell element. This quadrilateral plate/shell element has been presented by combination of the quadrilateral membrane element, RQ4, [18] and a quadrilateral discrete Kirchhoff plate bending element, DKQ8. Later on, 5-node (pentagonal) discrete Kirchhoff flat shell element with 20 dof, DKP20, was obtained directly by the superposition of the membrane element (RP5) with 10 dof and the discrete Kirchhoff plate bending element (DKP10) with 10 dof by Batoz and coworkers [6].

A similar 5-node flat shell element with 30 dof has not been developed so far to our knowledge. The purpose of this research work is, therefore, to present a 5-node plate/shell element named DKP30 by combination of the 5-node membrane element (RP15) with drilling dof and the refined 5-node discrete Kirchhoff plate bending element (DKP15) with 15 dof (Fig.1) [1]. In the following sections the details of the formulation of the DKP30 flat shell element were presented.

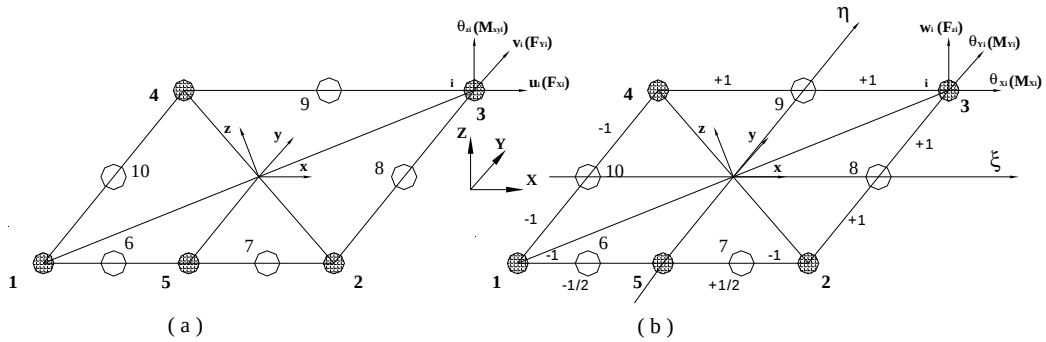

Fig.1. Five-node DKP30 flat shell element. a) membrane b) discrete Kirchhoff plate

2. The formulation of shell element

Figure 1 shows 5-node shell element with the combination of the membrane (Fig. 1.a) and the plate (Fig. 1.b) elements. In these figures, general coordinate axes are denoted by X, Y, Z with $(u, v, w, \theta_x, \theta_y, \theta_z)$ degrees of freedom while x, y, z show the local coordinate frame. In these definitions u, v and w are the displacements defined on the X, Y and Z axes while θ_x, θ_y and θ_z are the positive rotations about the same axes, respectively.

2.1 The formulation of membrane element with drilling degree of freedom

The Lagrangian shape functions of 5-node membrane element in the natural coordinates can be written as

$$
\begin{aligned}
N_1 &= N_1^0 - \frac{3}{8}N_6 + \frac{1}{8}N_7 - \frac{1}{2}N_{10} & N_1^0 &= \frac{1}{4}(1-\xi)(1-\eta) - \frac{1}{2}N_5^0 & N_6 &= \frac{4}{3}\xi(1-\xi^2)(\xi-0.5)(1-\eta)\\
N_2 &= N_2^0 - \frac{3}{8}N_7 + \frac{1}{8}N_6 - \frac{1}{2}N_8 & N_2^0 &= \frac{1}{4}(1+\xi)(1-\eta) - \frac{1}{2}N_5^0 & N_7 &= \frac{4}{3}\xi(1-\xi^2)(\xi+0.5)(1-\eta)\\
N_3 &= N_3^0 - \frac{1}{2}(N_8+N_9) & N_3^0 &= \frac{1}{4}(1+\xi)(1+\eta) & N_8 &= \frac{1}{2}(1+\xi)(1-\eta^2)\\
N_4 &= N_4^0 - \frac{1}{2}(N_9+N_{10}) & N_4^0 &= \frac{1}{4}(1-\xi)(1+\eta) & N_9 &= \frac{1}{2}(1-\xi^2)(1+\eta)\\
N_5 &= N_5^0 - \frac{3}{4}(N_6+N_7) & N_5^0 &= \frac{1}{2}(1-\xi^2)(1-\eta) & N_{10} &= \frac{1}{2}(1-\xi)(1-\eta^2)
\end{aligned}
\qquad (1)
$$

where $(N_i, i = 1,2,3,4,5)$ is the shape function of the 5-node element

From virtual work equation the following classical formulations are obtained.

$$\begin{Bmatrix} F_{Xi} \\ F_{Yi} \\ M_{XYi} \end{Bmatrix} = \begin{Bmatrix} Q^T F_{xi} \\ Q^T F_{yi} \\ Q^T M_{xyi} \end{Bmatrix} = \left[Q^T K_d Q \right] . \begin{Bmatrix} u_i \\ v_i \\ \theta_{Zi} \end{Bmatrix} = \left[K_D \right] . \begin{Bmatrix} u_i \\ v_i \\ \theta_{Zi} \end{Bmatrix}, i = 1,2,3,4,5 \tag{2}$$

where

$$\left[K_d \right] = \int_A \left[\overline{B}_d \right]^T \left[D_d \right] \left[\overline{B}_d \right] dA \tag{3}$$

$$\left[Q \right] = \begin{bmatrix} e_{11} & e_{12} & e_{13} \\ e_{21} & e_{22} & e_{23} \\ e_{31} & e_{32} & e_{33} \end{bmatrix}, \quad \left[D_d \right] = \frac{Et}{1-\nu^2} \begin{bmatrix} 1 & \nu & 0 \\ \nu & 1 & 0 \\ 0 & 0 & \dfrac{1-\nu}{2} \end{bmatrix} \tag{4}$$

$$\left[\overline{B}_d \right] = \begin{Bmatrix} \partial N_i^0 / \partial x & 0 & 0 & 0 & 0 & G_i \\ 0 & \partial N_i^0 / \partial y & 0 & 0 & 0 & G_i \\ \partial N_i^0 / \partial y & \partial N_i^0 / \partial x & 0 & 0 & 0 & G_i \end{Bmatrix} \tag{5}$$

$$\left[G_i \right] = \frac{1}{8} \begin{Bmatrix} L_{ij} C_{ij} \dfrac{\partial N_l}{\partial x} - L_{ik} C_{ik} \dfrac{\partial N_m}{\partial x} \\ L_{ij} S_{ij} \dfrac{\partial N_l}{\partial y} - L_{ik} S_{ik} \dfrac{\partial N_m}{\partial y} \\ \left(L_{ij} C_{ij} \dfrac{\partial N_l}{\partial y} - L_{ik} C_{ik} \dfrac{\partial N_m}{\partial y} \right) - \left(L_{ij} S_{ij} \dfrac{\partial N_l}{\partial x} - L_{ik} S_{ik} \dfrac{\partial N_m}{\partial x} \right) \end{Bmatrix} \tag{6}$$

and E is modulus of elasticity, t is the shell thickness, ν is the poisson ratio, $[Q]$ is the transformation matrix between the global and local cartesian coordinates, $[D_d]$ is the elastic material constants matrix for plane stress case, $\left[K_d \right]$ is the local stiffness matrix, and $\left\{ e_{ij} \right\} (i,j=1,2,3)$ are the direction cosines between two coordinate frames. Moreover, G_i is valid for only $i = 1,2,3,4,5$ whereas the other indices take the values of $j = 4, 5, 2, 3, 1$, $k = 5, 3, 4, 1, 2$, $l = 10, 7, 8, 9, 6$ and $m = 6, 8, 9, 10, 7$.

2.2 The formulation of discrete Kirchhoff Plate Bending Element

Because of the C^0-continuity requirement, compatible displacement 5-node elements based on the Kirchhoff thin plate theory are very difficult to formulate. In order to develop a 5-node discrete Kirchhoff plate bending element, DKP, an alternative expansion of discrete Kirchhoff element approach are used here. The elements obtained by this method satisfies C^1 continuity requirement on the element boundary and applied to triangular [DKT6, DKT9, IDKT, DKT-BK, RDKT, DKTP, DKL, DKTL, etc] and quadrilateral plate elements [DKQ, SLICK, DKQ8, IDKQ, RDKQ, DKQP, Semiloof, etc].

The functional in deriving the element stiffness matrix of a Kirchhoff plate can be given as

$$p = \frac{1}{2}\int_{V_e} k^t D_b k dv \tag{7}$$

where k and D_b are the matrix of curvatures of the element and the elasticity matrix, respectively and can be defined as

$$k = \begin{Bmatrix} \dfrac{\partial q_x}{\partial x} \\ \dfrac{\partial q_y}{\partial y} \\ \dfrac{\partial q_x}{\partial y} + \dfrac{\partial q_y}{\partial x} \end{Bmatrix}, \quad D_b = \frac{Eh^3}{12(1-n^2)} \begin{bmatrix} 1 & n & 0 \\ n & 1 & 0 \\ 0 & 0 & 0.5(1-n) \end{bmatrix} \tag{8}$$

Let us now define the rotations q_x and q_y in order to obtain the formulas for a new Kirchhoff plate element as

$$\begin{aligned} q_x &= \sum_{i=}^{10} N_i q_{xi} \\ q_y &= \sum_{i=}^{10} N_i q_{yi} \end{aligned} \tag{9}$$

where N_i are the shape functions of the 5-node element in the natural coordinates. In order to derive 5-node element as shown in Fig. 2-a, the additional parameters q_{xj} and q_{yj} at the mid-node of the element boundary as shown in Fig. 2-b can be eliminated by the use of the interpolation functions of the boundary displacements.

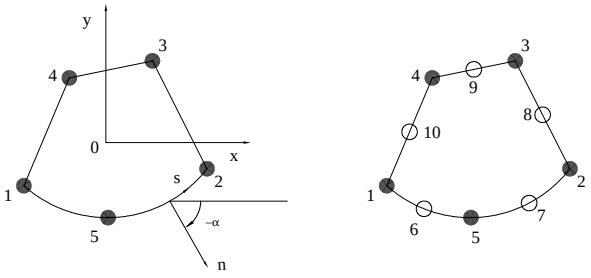

(a) (b)

Fig. 2. Plate bending element. a) 5-node element, b) 10-node element

For example, the interpolations of displacements, $\tilde{q}_n$ and $\tilde{q}_s$, along the boundary 5-2, which are linear and quadratic, respectively, are derived by using the parameters q_{ni}, q_{si}, and w_i $(i = 5,2)$. They can then be expressed as,

$$\tilde{q}_n = L_5 q_{n5} + L_2 q_{n2} \tag{10}$$

$$\tilde{q}_s = -(6L_5L_2/L)w_5 + L_5(L_5 - 2L_2)q_{s5} + (6L_5L_2/L)w_2 + L_2(L_2 - 2L_5)q_{s2} \tag{11}$$

where q_{nj} and q_{sj} are the slopes at nodes $j(j = 5,2)$ for the normal and tangential directions, respectively. Moreover, $\tilde{q}_s$ is based on the fact that the deflection w_i on the same boundary should be cubic. L_{52}, is the length of 5–2 boundary and $L_5 = 1 - s/L_{52}$ and $L_2 = s/L_{52}$ in which s is the coordinate along the boundary (Fig. 2-a). q_{n7} and q_{s7} at the mid-node 7 on the element boundary 5-2 are determined by substituting the values $L_5 = L_2 = 0.5$ into Eqs. (10) and (11) as

$$q_{n7} = \frac{1}{2}(q_{n5} + q_{n2}) \tag{12}$$

$$q_{s7} = -\frac{1.5}{L_{52}}w_5 - \frac{1}{4}q_{s5} + \frac{1.5}{L_{52}}w_2 - \frac{1}{4}q_{s2} \tag{13}$$

At any point on the boundary, the relation between q_{nj}, q_{sj} and q_{xj}, q_{yj} can be given as follows:

$$\begin{Bmatrix} q_{nj} \\ q_{sj} \end{Bmatrix} = \begin{bmatrix} l & m \\ -m & l \end{bmatrix} \begin{Bmatrix} q_{xj} \\ q_{yj} \end{Bmatrix} \tag{14}$$

in which *l* and *m* are the direction cosines of the boundary. The expression for the mid-node 7 on the boundary can be calculated by substituting Eq. (14) at $j = 5,7,2$ into Eqs. (12) and (13) as

$$\begin{Bmatrix} q_{x7} \\ q_{y7} \end{Bmatrix} = T_7 \begin{Bmatrix} w_5 \\ q_{x5} \\ q_{y5} \\ w_2 \\ q_{x2} \\ q_{y2} \end{Bmatrix} \tag{15}$$

where $T_7 = \begin{bmatrix} T_7^1 & T_7^2 \end{bmatrix}$ is called cyclic permutation matrix and given as

$$T_7^1 = \begin{bmatrix} 1.5m_2/L_{52} & -0.25m_2^2 + 0.5l_2^2 & 0.75l_2m_2 \\ -1.5l_2/L_{52} & 0.75l_2m_2 & -0.25l_2^2 + 0.5m_2^2 \end{bmatrix}$$
$$T_7^2 = \begin{bmatrix} -1.5m_2/L_{52} & -0.25m_2^2 + 0.5l_2^2 & 0.75l_2m_2 \\ 1.5l_2/L_{52} & 0.75l_2m_2 & -0.25l_2^2 + 0.5m_2^2 \end{bmatrix} \tag{16}$$

Hence

$$\begin{Bmatrix} q_{x7} \\ q_{y7} \end{Bmatrix} = A_2 q \tag{17}$$

where

$$A_2 = \begin{bmatrix} 0 & 0 & 0 & -1.5m_2/L_{52} & -0.25m_2^2 + 0.5l_2^2 & 0.75l_2m_2 & 0 \\ 0 & 0 & 0 & 1.5l_2/L_{52} & 0.75l_2m_2 & -0.25l_2^2 + 0.5m_2^2 & 0 \\ 0 & 0 & 0 & 0 & 0 & 1.5m_2/L_{52} & -0.25m_2^2 + 0.5l_2^2 \\ 0 & 0 & 0 & 0 & 0 & -1.5l_2/L_{52} & 0.75l_2m_2 \end{bmatrix} \tag{18}$$

$$q = \begin{bmatrix} w_1 & q_{x1} & q_{y1} & w_2 & q_{x2} & q_{y2} & w_3 & q_{x3} & q_{y3} & w_4 & q_{x4} & q_{y4} & w_5 & q_{x5} & q_{y5} \end{bmatrix}^T \tag{19}$$

The expressions for the rotations of the rest of the mid-nodes at $j = 6,8,9,10$ are obtained in a similar fashion by using cyclic permutation matrix $T_j\,(j = 6,8,9,10)$ and given in terms of the nodal parameters (w_j, q_{xj}, q_{yj}) for $j = 1,2,3,4,5$ as follows:

$$\begin{Bmatrix} \theta_{x6} \\ \theta_{y6} \end{Bmatrix} = A_1 q,\ \begin{Bmatrix} \theta_{x8} \\ \theta_{y8} \end{Bmatrix} = A_3 q,\ \begin{Bmatrix} \theta_{x9} \\ \theta_{y9} \end{Bmatrix} = A_4 q \text{ and } \begin{Bmatrix} \theta_{x10} \\ \theta_{y10} \end{Bmatrix} = A_5 q \tag{20}$$

where

$$A_1 = \begin{bmatrix} 1.5m_1/L_{15} & -0.25m_1^2 + 0.5l_1^2 & 0.75l_1m_1 & 0 & 0 & 0 & 0 \\ -1.5l_1/L_{15} & 0.75l_1m_1 & -0.25l_1^2 + 0.5m_1^2 & 0 & 0 & 0 & 0 \\ 0 & 0 & 0 & -1.5m_1/L_{15} & -0.25m_1^2 + 0.5l_1^2 & 0.75l_1m_1 & \\ 0 & 0 & 0 & 1.5l_1/L_{15} & 0.75l_1m_1 & -0.25l_1^2 + 0.5m_1^2 & \end{bmatrix} \tag{21}$$

$$A_3 = \begin{bmatrix} 0 & 0 & 0 & 1.5m_3/L_{23} & -0.25m_3^2 + 0.5l_3^2 & 0.75l_3m_3 & -1.5m_3/L_{23} \\ 0 & 0 & 0 & -1.5l_3/L_{23} & 0.75l_3m_3 & -0.25l_3^2 + 0.5m_3^2 & 1.5l_3/L_{23} \\ -0.25m_3^2 + 0.5l_3^2 & 0.75l_3m_3 & 0 & 0 & 0 & 0 & 0 \\ 0.75l_3m_3 & -0.25l_3^2 + 0.5m_3^2 & 0 & 0 & 0 & 0 & 0 \end{bmatrix} \tag{22}$$

$$A_4 = \begin{bmatrix} 0 & 0 & 0 & 0 & 0 & 0 & 1.5m_4/L_{34} & -0.25m_4^2 + 0.5l_4^2 & 0.75l_4m_4 \\ 0 & 0 & 0 & 0 & 0 & 0 & -1.5l_4/L_{34} & 0.75l_4m_4 & -0.25l_4^2 + 0.5m_4^2 \\ -1.5m_4/L_{34} & -0.25m_4^2 + 0.5l_4^2 & 0.75l_4m_4 & 0 & 0 & 0 & & & \\ 1.5l_4/L_{34} & 0.75l_4m_4 & -0.25l_4^2 + 0.5m_4^2 & 0 & 0 & 0 & & & \end{bmatrix} \tag{23}$$

$$A_5 = \begin{bmatrix} -1.5m_5/L_{41} & -0.25m_5^2 + 0.5l_5^2 & 0.75l_5m_5 & 0 & 0 & 0 & 0 \\ 1.5l_5/L_{41} & 0.75l_5m_5 & -0.25l_5^2 + 0.5m_5^2 & 0 & 0 & 0 & 0 \\ 0 & 0 & 1.5m_5/L_{41} & -0.25m_5^2 + 0.5l_5^2 & 0.75l_5m_5 & 0 & 0 \\ 0 & 0 & -1.5l_5/L_{41} & 0.75l_5m_5 & -0.25l_5^2 + 0.5m_5^2 & 0 & 0 \end{bmatrix} \tag{24}$$

The complete formulations of the element rotations for bending strain of the 5-node plate element DKP are determined by substituting Eqs. (17)– (24) into Eq. (9) as follows:

$$\begin{Bmatrix} q_x \\ q_y \end{Bmatrix} = \sum_{i=1}^{5} N_i \begin{Bmatrix} q_{xi} \\ q_{yi} \end{Bmatrix} + \sum_{i=1}^{5} N_{i+5} A_i q = \overline{N} q \tag{25}$$

where

$$\overline{N} = \begin{bmatrix} N_1^* & N_2^* & N_3^* & N_4^* & N_5^* \end{bmatrix} \text{ and } N_j^* = \begin{bmatrix} P_j & P_{xj} & P_{yj} \\ Q_j & Q_{xj} & Q_{yj} \end{bmatrix} \quad (j = 1,2,3,4,5)$$

$$\begin{aligned} P_1 &= 1.5\left(m_1 N_6 / L_{15} - m_5 N_{10} / L_{41}\right) \\ P_{x1} &= -0.75\left(m_1^{\,2} N_6 + m_5^{\,2} N_{10}\right) + N_1 \\ P_{y1} &= 0.75\left(l_1 m_1 N_6 + l_5 m_5 N_{10}\right) \end{aligned} \tag{26}$$

$$\begin{aligned} Q_1 &= 1.5\left(-l_1 N_6 / L_{15} + l_5 N_{10} / L_{41}\right) \\ Q_{x1} &= 0.75\left(m_1 l_1 N_6 + m_5 l_5 N_{10}\right) \\ Q_{y1} &= -0.75\left(l_1^{\,2} N_6 + l_5^{\,2} N_{10}\right) + N_1 \end{aligned} \tag{27}$$

and

$$l_1 = \frac{y_{51}}{L_{15}},\ m_1 = \frac{x_{51}}{L_{15}},\ l_5 = \frac{y_{14}}{L_{41}},\ m_5 = \frac{x_{14}}{L_{41}}$$

Next thing is now to form the element stiffness matrix. This can be achieved from the element displacement matrix shown in Eq. (25) by using the well known displacement finite element method and can then be expressed as follows:

$$\left[{}^{K}K_e\right] = \int_A \left[{}^{K}B_e\right]^T \left[D_e\right] \left[{}^{K}B_e\right] dA \tag{28}$$

$$\begin{aligned} \left[{}^{K}B_e\right] = &\begin{Bmatrix} 0 & 0 & 0 & 0 & -N_{1,i} & 0 \\ 0 & 0 & 0 & N_{2,i} & 0 & 0 \\ 0 & 0 & 0 & -N_{2,i} & N_{1,i} & 0 \end{Bmatrix} \\ &+ \begin{Bmatrix} 0 & 0 & {}^{K}A_{1,i}^{3,x} & {}^{K}A_{1,i}^{4,x} & {}^{K}A_{1,i}^{5,x} & 0 \\ 0 & 0 & {}^{K}A_{2,i}^{3,y} & {}^{K}A_{2,i}^{4,y} & {}^{K}A_{2,i}^{5,y} & 0 \\ 0 & 0 & \left({}^{K}A_{2,i}^{3,x} + {}^{K}A_{1,i}^{3,y}\right) & \left({}^{K}A_{2,i}^{4,x} + {}^{K}A_{1,i}^{4,y}\right) & \left({}^{K}A_{2,i}^{5,x} + {}^{K}A_{1,i}^{5,y}\right) & 0 \end{Bmatrix} \end{aligned} \tag{29}$$

where $[D_e]$ is the elastic bending stiffness matrix and the values for functions ${}^{K}A_{ndm,i}^{ndf,x(y)}$ are given in reference 1. The relation between the force and displacement is given as follows.

$$\begin{Bmatrix} F_{Zi}^e \\ M_{Xi}^e \\ M_{Yi}^e \end{Bmatrix} = \begin{Bmatrix} Q^T F_{zi} \\ Q^T M_{xi} \\ Q^T M_{yi} \end{Bmatrix} = \left[Q^T\, {}^{K}K_e Q\right] \cdot \begin{Bmatrix} w_i \\ \theta_{Xi} \\ \theta_{Yi} \end{Bmatrix} = \left[{}^{K}K_E\right] \begin{Bmatrix} w_i \\ \theta_{Xi} \\ \theta_{Yi} \end{Bmatrix} \tag{30}$$

3. The stiffness matrix of 5-node shell element

The stiffness matrix for 5-node shell element in global coordinates was obtained by superposing the stiffness matrices of membrane and bending elements. 3x3 Gauss integration points are used for the solutions of the all equations.

4. Numerical examples

The derived element formulation has then been implemented in an extended version of the general purpose finite element program FEAP [19] to develop 30-dof DKP30 element for the finite element analysis of plate/shell problems. In order to test the robustness, accuracy and efficiency of the DKP30 flat shell element, a number of well-known benchmark tests [20,21] are applied to a set of plate and shell problems and some of them are given in the following sections.

4.1. Membrane and bending patch test

A rectangular plate under membrane forces and bending moments was investigated according to [20]. Fig. 3 shows the mesh, geometry and the material properties of the plate element. The coordinates of nodal points for the element are given in Table 1 while the loading and boundary conditions are tabulated in Table 2. The numerical results obtained for the patch test are also tabulated in Table 3 while Fig. 4 illustrates the rotation distribution about Y axis at constant bending loading. The results showed that the present element passed the patch test under both the membrane and bending loading conditions.

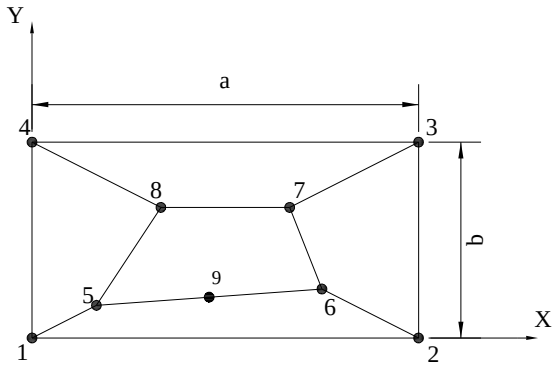

a=0.24; b=0.12; t=0.001; E=10^6; υ=0.25

Fig. 3. Meshing for the Patch test of the DKP30 flat shell element

Table 1. Nodal coordinates for nodes of the DKP30 flat shell element

Node	X	Y
1	0.00	0.00
2	0.24	0.00
3	0.24	0.12
4	0.00	0.12
5	0.04	0.02
6	0.18	0.03
7	0.16	0.08
8	0.08	0.08
9	0.11	0.025

Table 2. Boundary and loading conditions for the Patch test

	BCs (1: fixed, 0: free)	Loads
Constant strain in X-direction	1: 1,1,1,0,0,1 2: 0,1,1,0,0,0 4: 1,0,1,0,0,0	2: $F_x = 0.06$; $M_z = -0.0012$ 3: $F_x = 0.06$; $M_z = 0.0012$
Constant strain in Y-direction	1: 1,1,1,0,0,1 2: 0,1,1,0,0,0 4: 1,0,1,0,0,0	3: $F_y = 0.12$; $M_z = -0.0048$ 4: $F_y = 0.12$; $M_z = 0.0048$ 2: $M_z = 0.0048$
Constant shear in X-Y plane	1: 1,1,1,0,1,1 4: 1,0,1,0,0,0	2: $F_x = -0.048$; $F_y = 0.024$ 3: $F_x = 0.048$; $F_y = 0.024$ 4: $F_y = -0.024$
Constant bending, My=8.889e-8	1: 1,1,1,1,1,1 2: 0,0,0,1,0,0 3: 0,0,0,1,0,0 4: 1,0,1,1,1,1	2: $M_y = 5.33\ 10^{-9}$ 3: $M_y = 5.33\ 10^{-9}$
Constant biaxial bending, My=3.333e-8	1: 1,1,1,1,1,1 2: 0,1,1,0,1,0 4: 1,0,1,1,0,1	2: $M_x = 2.\ 10^{-9}$ 3: $M_x = 2.\ 10^{-9}$ 3: $M_y = -4.\ 10^{-9}$ 4: $M_y = -4.\ 10^{-9}$

Table 3. Patch test results obtained for the DKP30 flat shell element

	Constant strain in X-direction [x10^{-4}]	Constant strain in Y-direction [x10^{-4}]	Constant shear in X-Y plane [x10^{-4}]	Constant Bending, [x10^{-4}]	Constant Biaxial Bending, [x10^{-4}]
DKQ24	u2 = 2.8932 u3 = 2.811	v3 = 1.2 v4 = 1.2	v3 = 2.4	$\theta 3_y$ = 2.3985	$\theta 3_x$ = 1.2057 w3 = 0.144
DKP30	u2 = 2.8514 u3 = 2.8109	v3 = 1.2 v4 = 1.2	v3 = 2.4	$\theta 3_y$ = 2.3985	$\theta 3_x$ = 1.2064 w3 = 0.144
ANSYS (Shell 63)	u2 = 2.43614 u3 = 2.36386	v3 = 1.2 v4 = 1.2	v3 = 2.4	$\theta 3_y$ = 2.3985	$\theta 3_x$ = 1.2285 w3 = 0.144

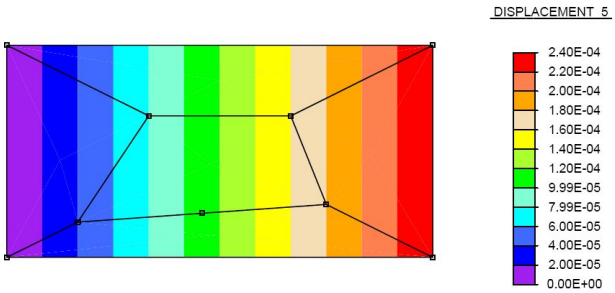

Fig. 4. Rotation $\left(\theta_y\right)$ distribution for the DKP30 flat shell element

4.2. Scordelis-Lo roof problem

The Scordelis-Lo roof problem provides a rigorous test of an element's ability to represent inextensional bending and complex states of membrane strains. Fig.5 represents a cylindrical roof supported by rigid diaphragms and loaded by its own weight. The material and geometrical data of the problem are also shown in Fig.5. Because of the double symmetry, only one quarter of the cylindrical roof is discretized and modeled with DKP30 elements. The displacement at the midside of the free edge, normalized with respect to the theoretical solution (w=0.3024) obtained by MacNeal and Harder [20], by taking the ratios of the deflections in Y-direction to the theoretical ones, was compared to the solutions of the other elements such as DKQ24 [1], SRI [22], MITCA4 [23], TRIC [17], Mixed [24], and QPH [25].

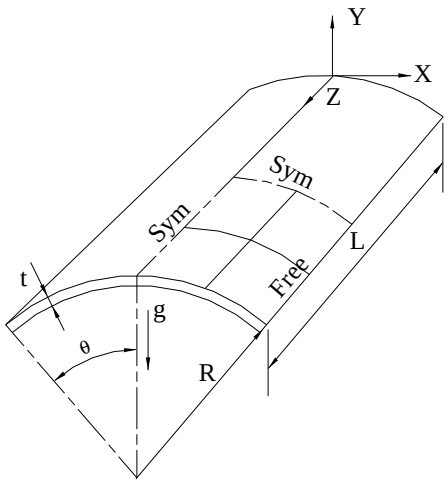

L=50; R=25; t=0.25; θ=40°; E=4.32x10^8
ρ=36.7347; g=9.8; $u_x = u_y = 0$ on curved edges

Fig. 5. Scordelis-Lo roof problem

The results of comparison were tabulated in Table 4 and showed that the DKP30 flat shell element had a better solution than that of TRIC element. The deflection distribution of DKP30 elements was presented in Fig. 6.

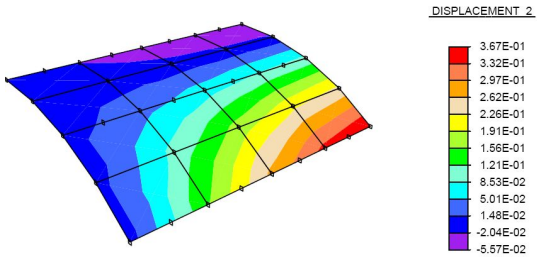

Fig. 6. Deflection distribution respect to Y-direction for the DKP30 flat shell element

Table 4. Deflection ratios in the Y-direction for Scordelis-Lo roof problem

Element type	v_{fem}/v_{exact}
SRI	0.964
MITCA4	0.940
Mixed	1.083
QPH	0.940
TRIC	0.697
DKQ24	1.128
DKP30	1.190

4.3. Pinched cylinder problem

Fig. 7 illustrates the benchmark problem of a cylindrical shell supported by two rigid diaphragms under the load of two opposing concentrated forces. In the pinched cylinder problem, shear locking is more severe than membrane locking. Due to the symmetry, one-eighth of the cylinder is modeled with 4x4 mesh.

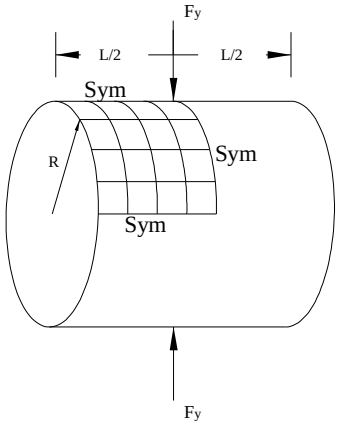

L=600, R=300; t=3; E=3.0x10^6; υ=0.3

Fig.7. Pinched cylinder roof problem

The deflection ratios obtained in Y-direction by using DKP30 elements for cylindrical shell problem are compared with the other elements available in the literature and given in the Table 5. It is clearly seen from the table that the closest solution to the theoretical one is obtained from the DKP30 elements. The deflection distributions of the DKP30 elements are shown in Fig. 8.

Table 5. Deflection ratios in the Y-direction for cylinder problem

Element type	v_{fem}/v_{exact}
SRI	0.373
RSDS	0.469
MITCA4	0.370
Mixed	0.399
QPH	0.370
TRIC	0.412
ANS6S	0.502
DKQ24	0.644
DKP30	0.650

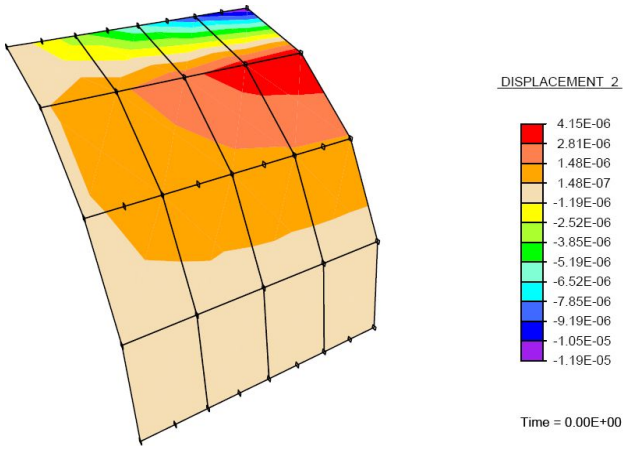

Fig. 8. Deflection distribution in the Y-direction for cylinder problem using the DKP30 element

4.4. Hemispherical shell problem

This problem consists of a thin hemisphere with four alternating point loads applied around the equator. The problem is illustrated in Fig. 9 with geometrical and material properties. Symmetry boundary conditions were applied to the appropriate outer edges of the quarter hemisphere model for simulation.

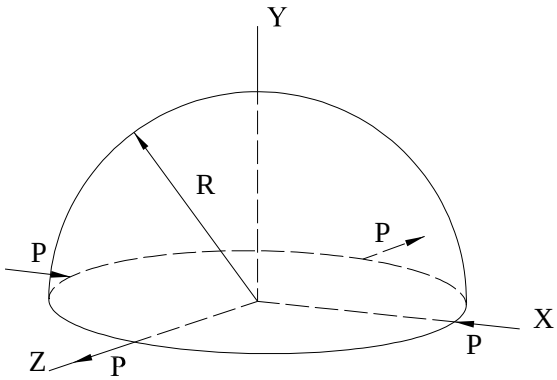

R=10; t=0.04; E=6.825x10^7; υ=0.3; P=2.0

Fig. 9. Hemishperical shell problem

The displacements in the X-direction are obtained and shown in Fig. 10 for hemispherical problem modeled by using DKP30 elements. The results are compared with the other elements available in the literature and given in the Table 6. This table clearly showed that the third best solution was obtained from the DKP30 elements by giving better solution from SRI, MITCA4, Mixed, QPH, and DKQ24 elements.

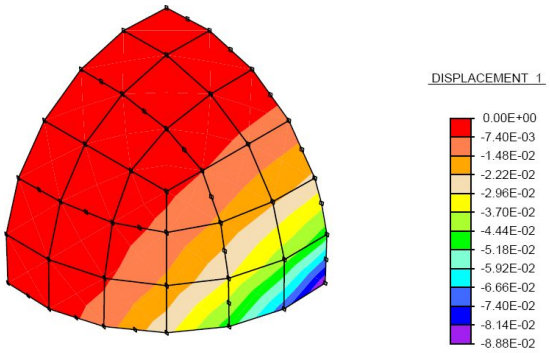

Fig. 10. Displacement distribution in the X-direction for hemisphere problem using DKP30 element

Table 6. Displacement ratio in the X-direction for hemisphere problem

Element type	u_{fem}/u_{exact}
SRI	0.412
RSDS	0.965
MITCA4	0.390
Mixed	0.651
QPH	0.280
TRIC	1.022
DKQ24	0.777
DKP30	0.961

4.5. Skew plate

Fig. 11 shows a uniformly loaded skew plate with its dimensions, material properties and the skew angle of β=40°. Mesh refinement was performed by starting from upper right end point (point A) where the maximum deflection occurs to the center of the plate. The results obtained for the deflection at point A using the both elements, DKQ24 and DKP30, are shown in Figure 12 and in Table 7. It is clearly seen from this table that the results are getting closer to the exact solution when both DKQ24 and DKP30 elements are used together than the results obtained from DKQ24 elements alone.

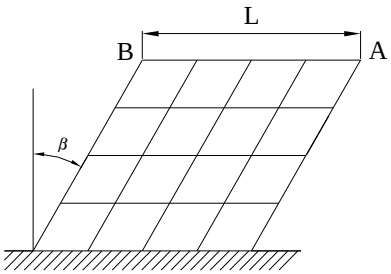

L=10; t=0.2; β=40°; E=200x10^9; υ=0.3, q=-1.0

Fig. 11. Skew cantilever plate with 4x4 mesh

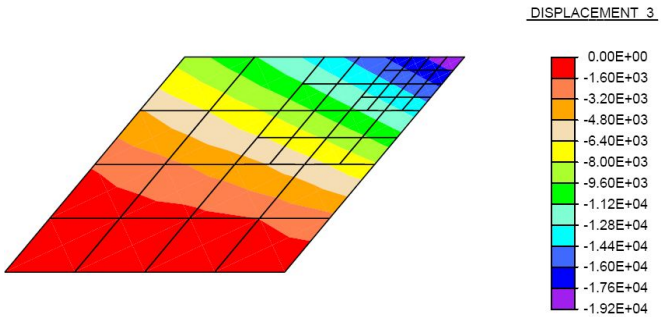

Fig.12. Deflection distribution for skew plate

Table 7. Deflection values for skew plate

Total element number	Deflection, $w_A/(Et^3/qL^4)$	Error (%)	Exact
4	1.4437 (DKQ24)	46.42	0.9894
16	1.2284 (DKQ24)	24.16	
64	1.1778 (DKQ24)	19.04	
28	1.1141 (DKQ24/DKP30)	12.64	
40	1.1125 (DKQ24/DKP30)	12.44	

5. Conclusion

In the present study, a derivation was pursued in order to develop the 5-node DKP30 flat shell element and an investigation was taken place to determine its accuracy and performance as well as its applicability as a transition element along with 4-node DKQ24 flat shell element. The results showed that DKP30 passed the patch test. The proposed element was then subjected to the known benchmark test problems and the results were compared to those of the different elements available in the literature. It is clearly seen from the comparison results that the acceptable convergence ratios and accuracies are obtained from the proposed element. Finally, it can be concluded from the skew plate examples that the proposed 5-node DKP30 element can be used along with the 4-node DKQ24 as a transition element where mesh refinement is necessary.

References

[1] Gedikli, H. *The Investigation of Flat Shell Elements by Using The Refined Finite Element Method*, Ph.D. Thesis, Karadeniz Technical University, Turkey, 2005 (in Turkish).

[2] Zhang, X.Y, Cheung Y.K., Chen, W.J. Two refined non-conforming quadrilateral flat shell elements, *Int J Num Meth Engng*, 49, 355-382, 2000.

[3] Batoz, J.L., Hammadi, Zheng, F., Zhong, C. On the linear analysis of plates and shells using a new-16 degrees of fredom flat shell element, *Computers and Structures,* 78, 11-20, 2000.
[4] Dawe, D.J. Shell analysis using a simple facet element, *J Strain Analysis,* 7, 266-270, 1972.
[5] Morley, L.S.D. The constant moment plate bending element, *J Strain Analysis,* 6, 20-24, 1971.
[6] Batoz, J.L, Zheng, C.L, Hammadi, F. Formulation and evaluation of new triangular, quadrilateral, pentagonal and hexagonal discrete Kirchhoff plate/shell elements, *Int J Num Meth Engng,* 52, 615-630, 2000.
[7] Batoz, J,L, Dhatt, G., Development of two simple shell elements. American Institute of Aeronautics and Astronautics, 10, 237-238, 1972.
[8] Bathe, K,J, Ho, L.W. A simple and effective element for the analysis of general shell structures", *Computers and Structures,* 13, 673-681, 1981.
[9] Carpenter, N., Stolarski, H., Belytschko, T. A flat triagular shell element with improved membrane interpolation", *Computer Methods in Applied Mechanics and Engineering,* 1, 161-168, 1985.
[10] Dhatt, G., Marcotte, L., Matte, Y., Talbot M. Two new discrete Kirchhoff plate shell elements, *4th Symposium on Numerical Methods in Engineering,* Atlanta, Georgia, 599-604, 1986.
[11] Fafard, M., Dhatt, G., Batoz, J.L. A new discrete Kirchhoff plate/shell element with updated procedures, *Computers and Structures,* 31, 591-606, 1989.
[12] Talbot, M., Dhatt, G. Three discrete Kirchhoff elements for shell analysis, with large geometrical non linearities and bifurcations, *Engineering Computations*, 4,415-22, 1987.
[13] Poulsen, P.N, Damkilde, L. A flat triangular shell element with loof modes, *Int J Num Meth Engng*, 39, 3867-3887, 1996.
[14] Samuelson, A. The global constant strain condition and the patch test, *Energy Methods in Finite Element Analysis*, Wiley: New York, 47-52, 1979.
[15] Felippa, C.A, Haugen, B. Militello, C. From the individual element test to finite element templates: evolution of patch test, *Int J Num Meth Engng,* 38, 199-229, 1995.
[16] Noor, A.K. Bibliography of monographs and surveys on shells, *Applied Mechanics Review,* 43, 223-224, 1990.
[17] Argyris, J.H, Papadrakkakis, M, Apostolopoulou, C., Koutsourelakis, S. The TRIC shell element: theoretical and numerical investication", *Computer Methods in Applied Mechanics and Engineering,* 182, 217-245, 2000.
[18] Zhong, W.X., Zeng, J. Rotational finite elements, *J Comp Struct Mech Appl*, 13, 1-8, 1996.
[19] Zienkiewicz, O.C, Taylor, R.L. *The Finite Element Method*, Vol.1-3, 5.ed. Butterworth-Heinemann, Oxford, 2000.
[20] MacNeal, R.H., Harder, R.L. A proposed standard set of problems to test finite element accuracy, *Finite Element Analysis and Design,* 1, 3-20, 1985.
[21] Green, S, Turkiyyah, G. Second Order Accurate Constraint Formulation for Subdivision Finite Element Simulation of Thin Shells, *Int J Num Meth Engng,* 61(3), 380-405, 2004.
[22] Huges, T.J.R., Liu, W.K. Nonlinear finite element analysis of shells, part II: two-dimensional shells, *Comp Meth Appl Mech Eng,* 27, 167-182, 1981.
[23] Bathe, K.J., Dvorkin, E.N. A formulation of general shell elements-the use of mixed interpolation of tensorial components, *Num Meth Eng,* 22, 697-722, 1986.

[24] Simo, J.C, Fox D.D. On a Stress Resultant Geometrically Exact Shell Model. Part II, The linear theory; computational aspects, *Comp Meth Appl Mech Eng*, 73, 53-92, 1989.
[25] Belytschko, T., Leviathan, I. Physical stabilization of the 4-node shell element with one point quadrature, *Comp Meth Appl Mech Eng*, 113, 321-350, 1994.